

The influence of basement structure on the evolution of the Bicornb-Quesa Diapir (eastern Betics, Iberian Peninsula): contractive thin-skinned deformation above a pre-existing extensional basement fault

M. Rubinat · E. Roca · M. Escalas ·
P. Queralt · O. Ferrer · J. J. Ledo

Received: 12 August 2011 / Accepted: 29 April 2012 / Published online: 29 May 2012
© Springer-Verlag 2012

Abstract On the basis of an analysis of structural surface data in addition to previously available and new magnetotelluric data, it was possible to reconstruct the evolution of Bicornb-Quesa Diapir. This was initiated as a reactive diapir in relation to a basement fault. The reactive diapir was rejuvenated by a thin-skinned compression during the Paleogene and rose during an extensional early-middle Miocene phase. Later, in the middle Miocene, the diapir was squeezed and then, in the late Miocene, was extensionally reactivated. The current reconstruction allows us to analyse a diapir affected by a thin-skinned contractional deformation located on top of a pre-existing basement fault. Our study highlights the role played by the geometric relationship between the propagation direction of the cover deformation and the basement fault.

Keywords Salt diapir · Rejuvenation · Contraction · Extension · Basement fault · Betics

Introduction

The influence of basement extension on an overburden detached above an evaporitic layer is well known (Nalpas and Brun 1993; Jackson and Vendeville 1994; Vendeville et al. 1995; Withjack and Callaway 2000; Dooley et al. 2003, 2005), as is the inversion of a basement fault with the

same configuration (Letouzey et al. 1995; Krzywiec 2004; Ferrer et al. 2012). Similarly, the effect of compression on a thin-skinned overburden (Coward and Stewart 1995; Sans and Koyi 2001) and the effect of a thin-skinned contraction on a previously existing diapir (Vendeville and Nilsen 1995; Roca et al. 2006; Callot et al. 2007; Dooley et al. 2009) have been documented. However, no studies have yet dealt with the structure produced by a contractive thin-skinned deformation above a pre-existing basement fault. Addressing this gap is one of the goals of this study, and the Bicornb-Quesa Diapir has proved an excellent structure for this purpose because it is located above an N-dipping basement fault (Rubinat et al. 2010) and between two thin-skinned foldbelts.

The Bicornb-Quesa Diapir is a well-studied diapir with a long deformation history. It was initiated with the formation of a drape fold and a subsequent reactive diapir above the basement fault. Thereafter, during the latest stages of the south Iberian Chain contractional deformation, the reactive diapir was rejuvenated (in the present paper). Later, the rejuvenated diapir rose during an early-middle Miocene extensional phase and was squeezed during the north propagation of the Betic contractional deformation (Roca et al. 1996, 2006). Finally, it was reactivated by means of a Late Miocene extension (Roca et al. 1996, 2006). As a result of this evolution, it constitutes an example of a salt diapir formed over a basement fault that was (1) rejuvenated when a contractional thin-skinned deformation propagated toward the hanging-wall block of the basement fault and (2) reactivated by cover deformations propagating in the opposite direction on the footwall block of the basement fault.

This polyphase deformation of the Bicornb-Quesa Diapir and of one of the other salt diapirs present in the eastern Prebetics foldbelt has been recognized for a long time and

M. Rubinat (✉) · E. Roca · M. Escalas · P. Queralt ·
O. Ferrer · J. J. Ledo
Group of Geodynamics and Basin Analysis,
Departament de Geodinàmica i Geofísica, Facultat de Geologia,
Institut GEOMODELS, Universitat de Barcelona,
08028 Barcelona, Spain
e-mail: mrubin@ub.edu

has been used to propose different models of diapir reactivation during later extension, shortening and strike-slip deformations (De Ruig 1992, 1995; Roca et al. 1996, 2006). However, these earlier studies did not take into account the pre-Cenozoic structure of the area and the underlying basement structure. Thus, although geophysical data indicate the presence of basement faults beneath several salt diapirs (Carbó 1982; Castaño and Carbó 1995; Rubinat et al. 2010), basement faulting was not taken into consideration. Only a purely thin-skinned extensional model was used to analyse the kinematic evolution of the diapirs.

In the present paper, we seek to improve our understanding of the relationships between the basement, salt diapir and overburden structures in the Bicornb-Quesa diapir area in an effort to shed light on the role played by a pre-existing basement fault in diapir evolution. On the basis of this analysis, a new kinematic scenario is proposed, highlighting the role played by previous basement faults in the

initiation and reactivation of salt diapirs driven by a thin-skinned contractional deformation.

Geological setting and a summary of the structural evolution

The Bicornb-Quesa Diapir is located in the northeastern zone of the Prebetics (Fig. 1), which belongs to the most external part of the NNW-oriented foreland fold-and-thrust belt of the Betic Chain (Blumenthal 1927; Vera 1983). The Prebetics crop out widely at the eastern end of the chain where it consists of a para-autochthonous Jurassic to Miocene carbonate cover detached from an Iberian basement made up of Lower Triassic detrital rock and Variscan-deformed rock of the Paleozoic (Vera 1983). This autochthonous Iberian basement dips a few degrees to the southeast and is cut by high-angle extensional faults in the basement (Carbó 1982; Castaño and Carbó 1995; Rubinat

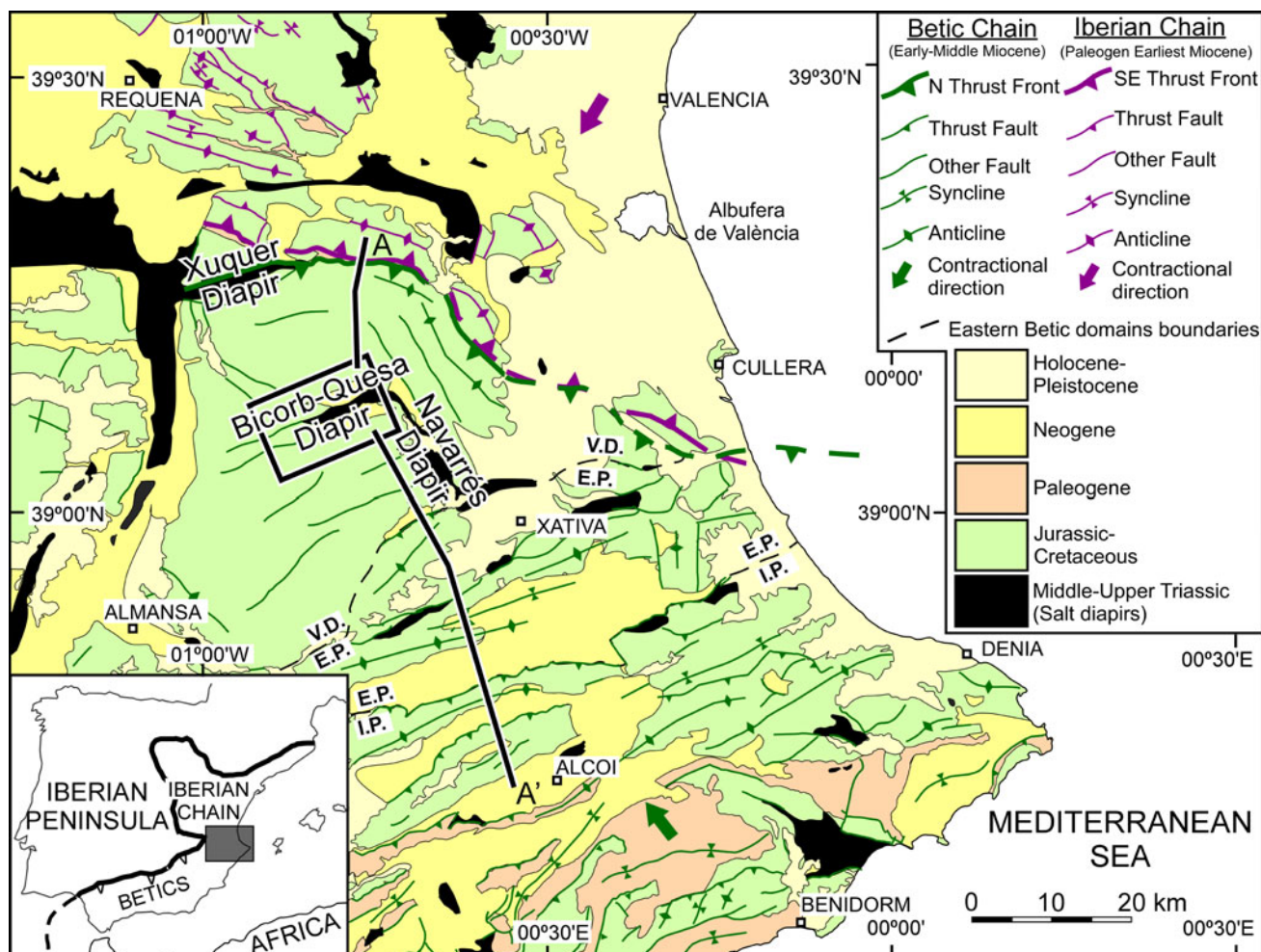


Fig. 1 Geological map of the eastern Prebetic Zone and adjoining southeastern part of the Iberian Chain (SE Spain). Note the different age and opposite sense of the deformation propagation in the Iberian

and Betic chains. I.P. means Internal Prebetic, E.P. External Prebetic and V.D. Valencian Domain. A–A': location of the cross section shown in Fig. 2. Black box location of study area (Fig. 3)

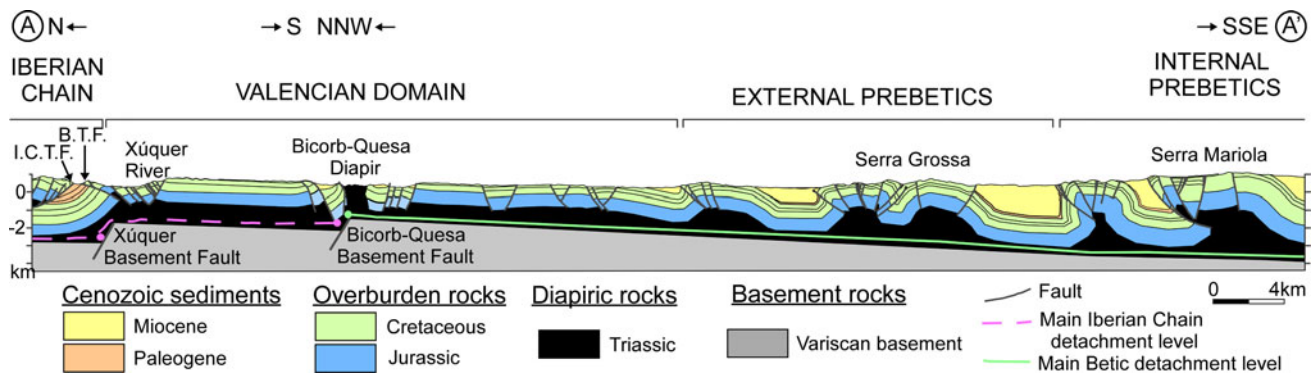


Fig. 2 Regional cross section depicting the main structural features of the Prebetic and Iberian Chain foreland fold-and-thrust belts (see location in Fig. 1). Note that N-dipping extensional fault basement

faults control the location both of salt diapirs and of thrust fronts (modified from Roca et al. 2006)

et al. 2010; ter Borgh et al. 2011). In contrast, above the detachment level (Middle-to-Upper Triassic evaporites), the Jurassic to Cenozoic (Miocene) cover is much more deformed with box-fold anticlines, steep dipping faults and salt diapirs cored by Triassic evaporites (Figs. 1, 2). The trend of these structures is predominantly ENE–WSW although other orientations are also present (De Ruig 1992; Roca et al. 2006; ter Borgh et al. 2011).

In this deformed cover, contractional deformation is predominant and decreases significantly toward the north-northwest. This results in a tapered geometry in cross section that thins north-northwestwards (Fig. 2). Recording the decrease in contractional deformation, three structural domains have been distinguished in the eastern Prebetics: the Internal Prebetics, the External Prebetics and the Valencian Domain (Fig. 1). (For details, interested readers can see García-Rodrigo 1960; Azéma et al. 1979; García-Hernández et al. 1980; De Ruig 1992; Roca et al. 2006.)

The overall structure of the eastern Prebetics reveals a complex deformation history. During the Jurassic, it was characterized by the opening of the Tethys passive margin and it was affected by salt diapirism probably driven by gravitational failure in the internal area (Martínez del Olmo 1999). Later, an early to middle Miocene extensional phase, which was related to the opening of the Valencia trough, generated a graben system (De Ruig 1992; Santisteban et al. 1994; Roca et al. 1996; Martínez del Olmo 1999; Roca et al. 2006) and led to the triggering and development of diapirs along the graben axes (Roca et al. 2006).

Over this pre-existing structure, the building of the Betic Chain resulted in the development of a thin-skinned fold-belt detached on the Middle-to-Upper Triassic salt layer, which, propagating to the northwest, led to the squeezing of the diapirs and the formation of complex contractional structures that linked them (Callot et al. 2007), the inversion of pre-existing faults, and to displacement to the north

above the evaporites of the Prebetics (Roca et al. 2006). After this contractional deformation, the entire structure was affected by a younger late Miocene extension episode that generated the extensional reactivation of some pre-existing overburden faults and diapirs (Ott d'Estevou et al. 1988; De Ruig 1995; Roca et al. 1996).

To complete this geological setting of the Bicorb-Quesa Diapir emplacement, it should be noted that the northern boundary of the eastern Prebetics (the northern edge of the Valencian Domain) coincides with the southwest frontal thrust of the Iberian Chain (Fig. 1). The Iberian Chain is an intraplate doubly vergent fold-and-thrust belt located in the central and eastern parts of the Iberian Peninsula (Fig. 1). It formed from the tectonic inversion of Late Permian–Early Cretaceous basins during the Paleogene–early Miocene times (Álvaro et al. 1979; Guimerà and Álvaro 1990) and, consequently, before the main contractional deformation of the eastern Prebetics. North of the study area, the Iberian Chain, consists of a system of SW-verging thrusts and folds, which was detached in the Middle–Upper Triassic evaporites and also pierced by salt diapirs (Moissenet 1985; Guimera et al. 2004). The southwest front of this system is located 15 km north of the Bicorb-Quesa Diapir and consists of a SW-verging thrust detached at the Middle–Upper Triassic evaporites (Fig. 2).

Stratigraphy

The Variscan basement is composed of Paleozoic sandstones, shales and quartzites that were metamorphosed and deformed between the Late Devonian and the Late Carboniferous Variscan orogeny (Bartrina et al. 1990; Martínez-Poyatos et al. 2004). Above the Variscan basement, the Permian to Lower Triassic sediments are mainly made up of synrift continental siliciclastic rocks that were deposited during the early stages of the extensional opening of the

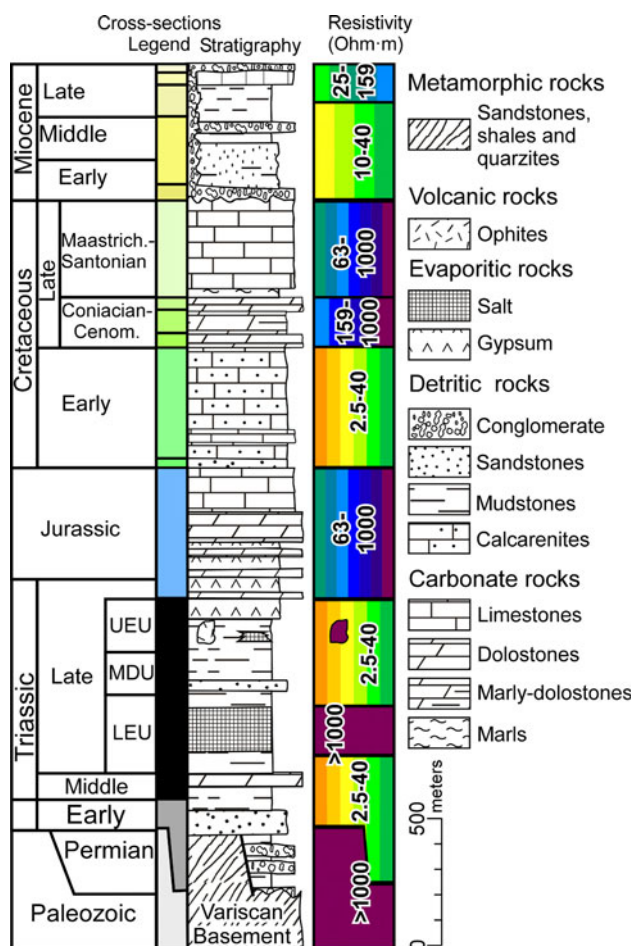


Fig. 3 Stratigraphic chart of the study area with the map and cross sections colour legend used for each differentiated unit, as well as the corresponding resistivity interval (modified from Rubinat et al. 2010)

Tethys Sea (Fig. 3) (Arche and López-Gómez 1996; Sopena and Sánchez-Moya 2004).

The Middle-to-Upper Triassic in the eastern Iberian plate is constituted by layered evaporite sequences with platform carbonates and fine-grained detrital interbeds. In the study area, it particularly consists of a thin basal evaporite layer (Röt facies), a 50–200 m thick succession of Middle Triassic carbonates (Fig. 3) (Muschelkalk facies; Suarez Alba 2007) and a 600–700 m thick succession of continental evaporites and fine clastics that are Upper Triassic in age (Keuper facies) (Bartrina et al. 1990; De Torres and Sánchez 1990). In this upper succession, salt is abundant and, on the basis of the predominant lithology, three stratigraphic units have been distinguished (Ortí 1974; Ortí and Salvany 1990): a *Lower Evaporite Unit*, formed by thick salt-layered sequences with thin interbeds of grey gypsiferous marls, sandstones and carbonates; a red *Mid-Detrital Unit*, composed of sandstones and mudstones; and an *Upper Evaporite Unit*, formed by salt, gypsum and red gypsiferous mudstones (Fig. 3).

On top of the ductile-deformed Middle-Upper Triassic, there is a 1500–1700 m thick overburden made up of a Jurassic-Cretaceous carbonate-dominated sequence (Meléndez 1979; Rios et al. 1980; García et al. 1981; Lanaja 1987). This overburden is unconformably overlain by Cenozoic terrigenous successions that crop out in the half-grabens (Fig. 3). Although some marine upper Oligocene to lowermost Miocene deposits are present locally, most of these Cenozoic successions are early-middle to late Miocene in age and were deposited in both alluvial and lacustrine environments (Santisteban et al. 1989; Anadón et al. 1998, 2000; Fig. 3).

The Bicornb-Quesa Diapir

The Bicornb-Quesa Diapir is an ENE-elongated salt diapir located in the central part of the Valencian Domain (Fig. 1). It is about 12 km long and widens progressively eastwards up to nearly 2 km in width at the eastern end of the diapir (Fig. 4). At that point, the Bicornb-Quesa Diapir joins the Navarrés Diapir, which spreads 15 km southwards following a NNW trend (Fig. 1). To the west, the Bicornb-Quesa Diapir termination coincides with the junction of the NW-trending Sácara Half-graben and the ENE-trending Juanera Half-graben (Fig. 5). These two half-grabens are in lateral continuity with the Bicornb and Quesa Half-grabens flanking the diapir and are also filled with Miocene deposits (Fig. 5).

The 3D structure of this diapir and the surrounding overburden and underlying basement have been analysed by means of detailed geological mapping (Fig. 4), the construction of a series of cross sections and the acquisition of two new magnetotelluric profiles (Fig. 6). Before describing this 3D structure, the main features and results of the new magnetotelluric survey are presented.

Bicornb-Quesa magnetotelluric data

The magnetotelluric (MT) method is a natural source electromagnetic (EM) technique that allows us to characterize the electrical conductivity distribution of the subsurface by simultaneously measuring the time variation of the electric and magnetic fields on the Earth's surface. The penetration of the electromagnetic field is a function of the electrical conductivity of the Earth (σ) and the frequency of the signal (f). The fundamentals of the method have been extensively presented by Vozoff (1991) and Simpson and Bahr (2005).

The use of the magnetotelluric technique to determine the deep structure of the study area is not new. Rubinat et al. (2010) performed a 2D magnetotelluric model of the Bicornb-Quesa diapir that revealed its main features at depth

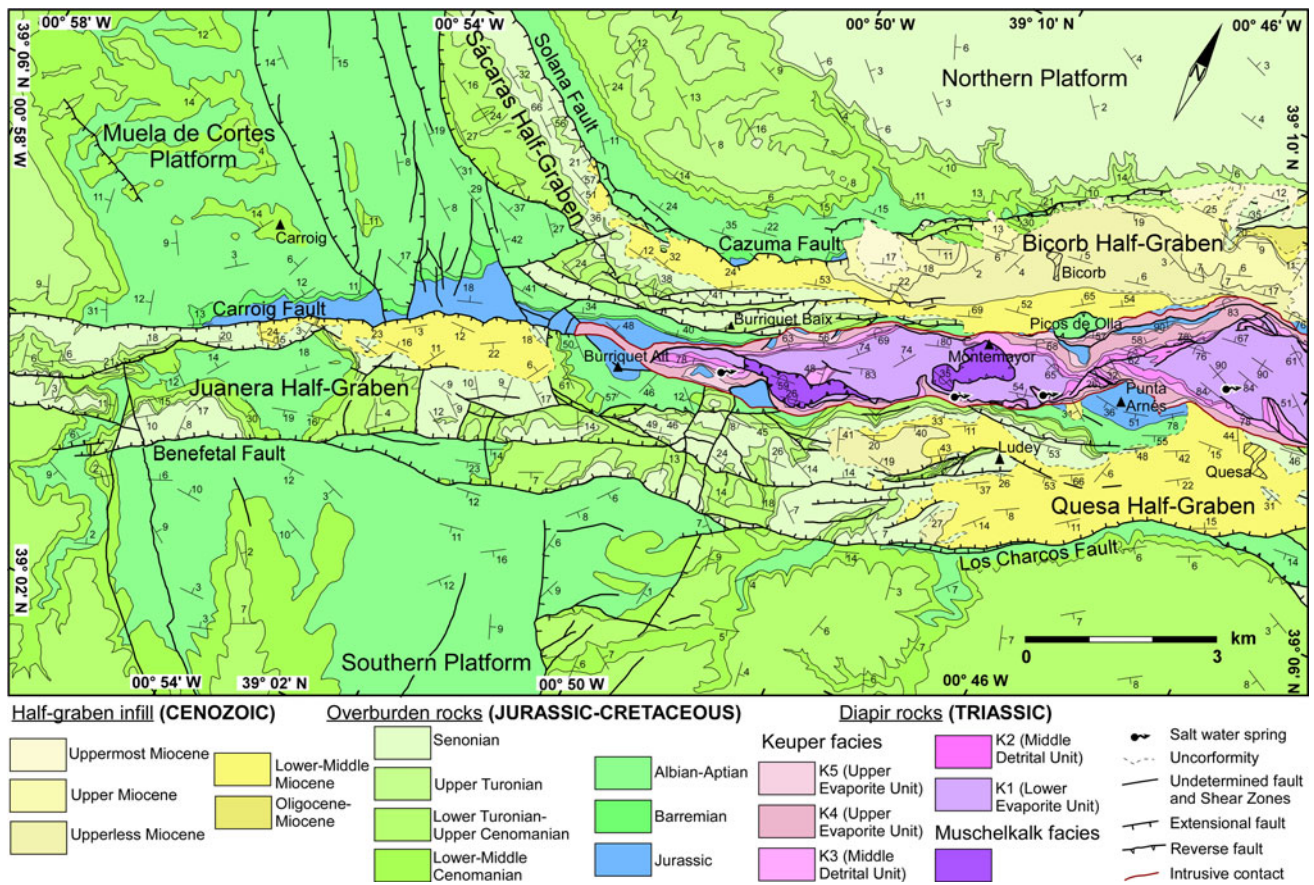


Fig. 4 Detailed geological map of the study area

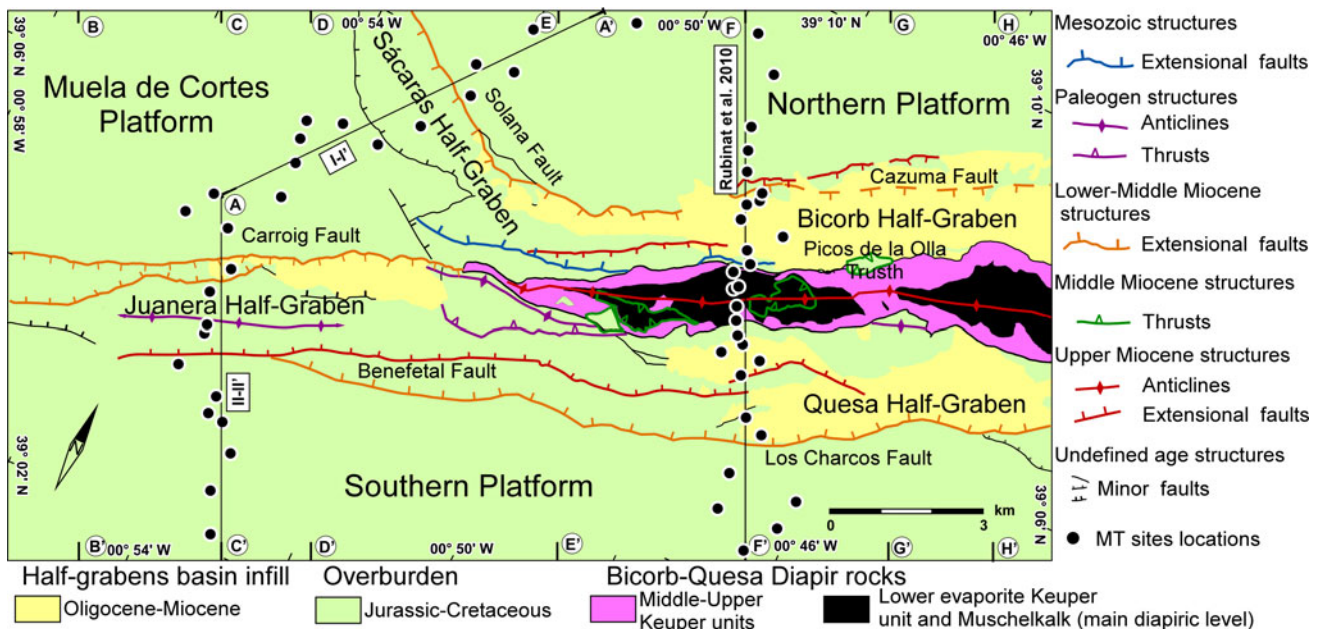


Fig. 5 Simplified geological map of the study area with the main Bicorb-Quesa Diapir and overburden structures. Paleogene, lower-middle and upper Miocene structures are differentiated to outline the

polydeformational history of the area. I–I', II–II' and Rubinat et al. (2010): location of the magnetotelluric models in Fig. 6; A–A' to H–H': location of the cross section in Fig. 7

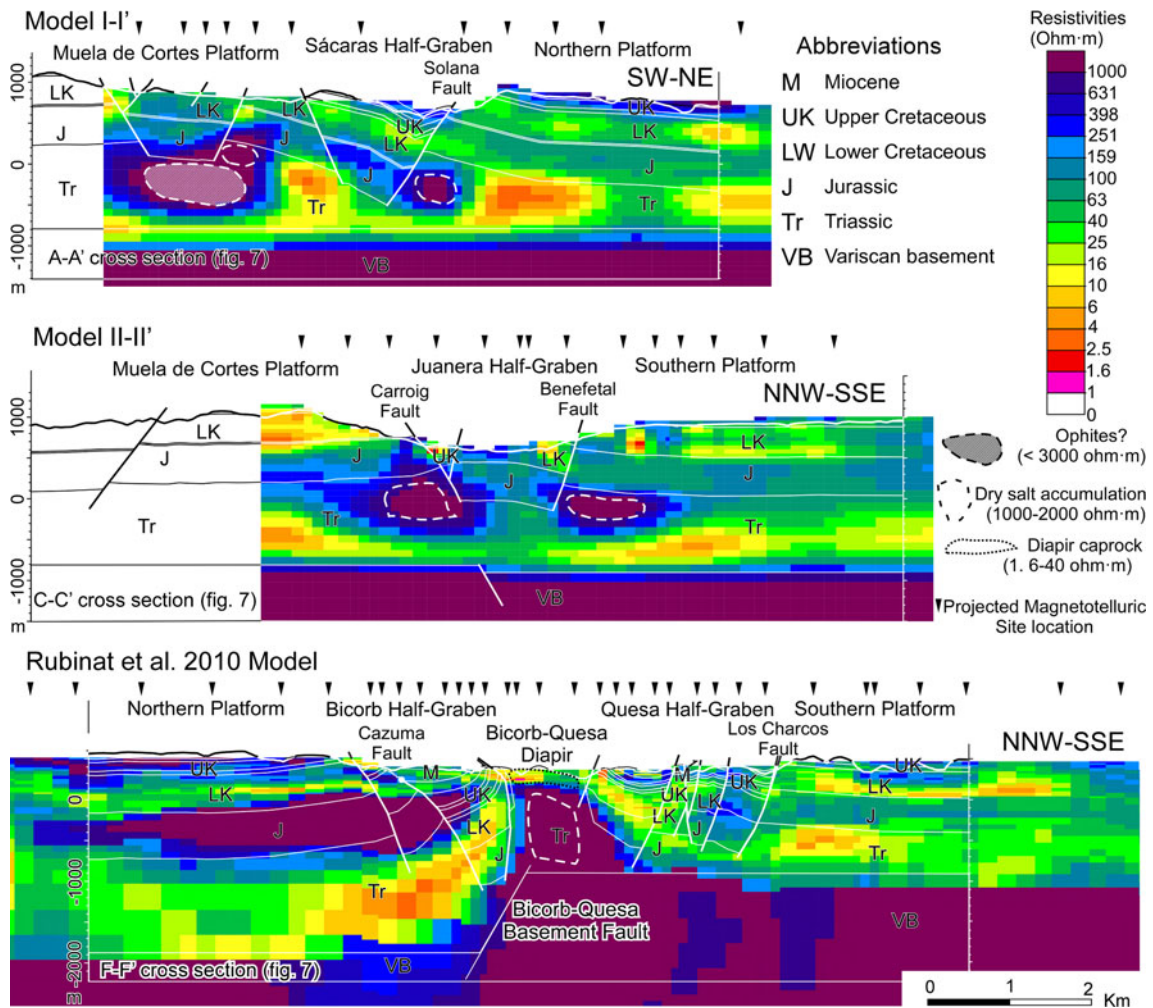


Fig. 6 2D Magnetotelluric models of the study area and Bicorb-Quesa Diapir (see Fig. 4 for location) with the Fig. 7 corresponding cross section. I-I' and II-II': new models through the Sácaras and Juanera Half-grabens. Rubinat et al. (2010): published model across

the Bicorb-Quesa Diapir and adjoining Bicorb and Quesa Half-grabens. The vertical elongated triangles represent the projected MT recorded stations

as well as those of the adjoining overburden and underlying basement. To create a more complete image of the subsurface structure, we carried out two new magnetotelluric profiles across the western part of the study area where the Bicorb-Quesa Diapir does not crop out (Fig. 4). These new models (I-I' and II-II' of Fig. 6) are based on the record of 26 new measuring stations (sites) using broadband ADU-06 MT stations from Metronix (Fig. 5). The sampling frequency ranged between 4096 and 2 Hz. To determine the direction of the geological structures (strike) and the TE and TM modes, we applied the McNeice-Jones (McNeice and Jones 2001) multi-site, multi-frequency MT tensor decomposition based on Groom and Bailey (1989).

As in Rubinat et al. (2010), the analysis of the dimensionality shows a regional 2D response within the range of 0.001–1 s, with some local distortion. The geoelectric strike direction of these predominant 2D structures is close

to N138° for model I-I' and N63° for the model II-II', which are perpendicular to the main outcropping geological structures.

In addition, the inversion of the acquired data in these new models points to significant resistivity contrasts in the bedrock, which, when combined with the geological cross sections obtained from field data, establishes a good correlation between resistivity and lithology (Fig. 3). In this correlation, the highest resistivity values fit in with dry evaporites (salt and anhydrites), basement metamorphic rocks, volcanic rocks and dolostones, the medium resistivity values correspond to limestones, and the lowest values fit in with mudstones, sandstones and wet evaporites (gypsum and wet salt) (Fig. 3). As a result, the MT models provide a lithostratigraphic image that substantially helps us to better understand the structure of the Bicorb-Quesa Diapir and surrounding areas, supplying information that

cannot be derived from the surface geology. The data allow us to recognize changes in Mesozoic stratigraphic thickness, determine the geometry of the basement top and decipher the motion and migration of the salt inside the diapiric rocks. In this regard, the Bicornb-Quesa MT models (Fig. 6) show the following:

1. The existence of an N-dipping extensional basement fault beneath the Bicornb-Quesa Diapir that was active during the sedimentation of both Permian-Lower Triassic and Upper Jurassic-Cretaceous successions (Rubinat et al. 2010).
2. The diapiric accumulation of Upper Triassic dry salt in the core of the Bicornb-Quesa Diapir (Rubinat et al. 2010) and a salt accumulation in the uplifted footwall of the main extensional faults, bounding the Juanera and Sácaras Half-grabens forming reactive diapirs (Vendeville and Jackson 1992).
3. The presence of an almost flat basement in the profiles that do not cross the diapir.

The Bicornb-Quesa structure

The structure of the Bicornb-Quesa area is strongly conditioned by the presence of a ductile and diapiric Middle-Upper Triassic level. This evaporite-detrital level decouples the deformation, resulting in a completely different structural style in the subsalt basement (thick-skinned) and supra-salt cover (thin-skinned) deformations (Nalpas and Brun 1993; Vendeville et al. 1995; Withjack and Callaway 2000; Dooley et al. 2005). The main features of these three different structural levels (subsalt basement, Middle-Upper Triassic detachment level and Jurassic to Miocene overburden) are detailed below.

Basement structure

Their resistivity signature (Fig. 6) and the available gravimetrics (Carbó 1980) indicate that the Variscan basement is cut by an ENE-trending fault below the outcropping Bicornb-Quesa Diapir. This fault, the Bicornb-Quesa Fault, sinks the NNW fault block with a vertical throw that decreases progressively westwards from about 1000 metres in the magnetotelluric profile until it disappears close to the western end of the present-day outcropping diapir (Rubinat et al. 2010). West of this location (Fig. 6), beneath the Juanera and Sácaras Half-grabens, the top of the Variscan basement appears nearly horizontal with a depth similar to the one observed in the SSE block of the Bicornb-Quesa Fault (900–1,000 m below sea level). The presence of a 100 m vertical throw and south dipping fault below the Carroig Fault can be observed (Fig. 6 Model II–II').

Above the Variscan basement top, the thickness and structure of the overlying Permian-Lower Triassic successions cannot be directly obtained from the available data. Both magnetotelluric and gravimetric data do not have enough resolution to distinguish these successions from the overlying Middle-Upper Triassic diapiric level. However, comparing the thickness of the “Triassic” conductor with the regional Middle-Upper Triassic thickness (about 600–800 m; Lanaja 1987; Bartrina et al. 1990), we can infer that it is relatively thick (400–500 m) in the hanging-wall of the Bicornb-Quesa Fault and very thin (<200 m) in the remaining areas. Such changes in thickness suggest a contemporaneous extensional motion of the Bicornb-Quesa basement fault similar to the motion described in other N- and E-trending basement faults of the Iberian Chain (Arche and Lopez-Gomez 1996; Arche et al. 2007).

Middle-Upper Triassic structure

The upper evaporite sequence constitutes the main décollement and source layer for diapirs in the eastern Iberian plate (Moissenet 1985; Guimerà and Álvaro 1990; De Ruig 1992; Martínez del Olmo 1999). However, as regards diapirism, it should be noted that it seems to be triggered mainly by the salt flow of the thick salt-layered sequences of the Lower Evaporite Unit (Fig. 3). In fact, although all the Middle-Upper Triassic units are present in the Bicornb-Quesa Diapir outcrop, surface mapping (Fig. 4) clearly shows that the dry salt coring the diapir correlates at the surface with the intensely folded and sheared sequences of the lower part of the Keuper facies (K1) as usually occurs in diapirs (Dooley et al. 2009).

The Bicornb-Quesa Diapir disappears progressively to the west and has a width of about 1 km except close to the junction of the Bicornb-Quesa and Navarrés Diapirs, where it attains a width of 2 km (Fig. 4). According to the magnetotelluric data (Rubinat et al. 2010), the cross-sectional shape of the salt wall is asymmetric, with the northern edge nearly vertical and the southern one dipping up to 50° to the south (Fig. 6). The internal structure of the salt wall is very complex with variably oriented folds, shear zones and faults that record a complex deformational history. However, the presence of a thrust with Muschelkalk materials above the diapir (Fig. 4) leads us to deduce that this structure occurred during a compressive stage prior to the placement of the diapir.

Outside the Bicornb-Quesa Diapir, the thickness of the Middle-Upper Triassic is rather constant below the overburden horizontal platforms but not beneath the half-grabens. Here, the Middle-Upper Triassic is much thinner beneath the hanging-wall blocks of the extensional faults but thicker in the footwall of the major half-graben bounding faults. This thickening is prominent along the

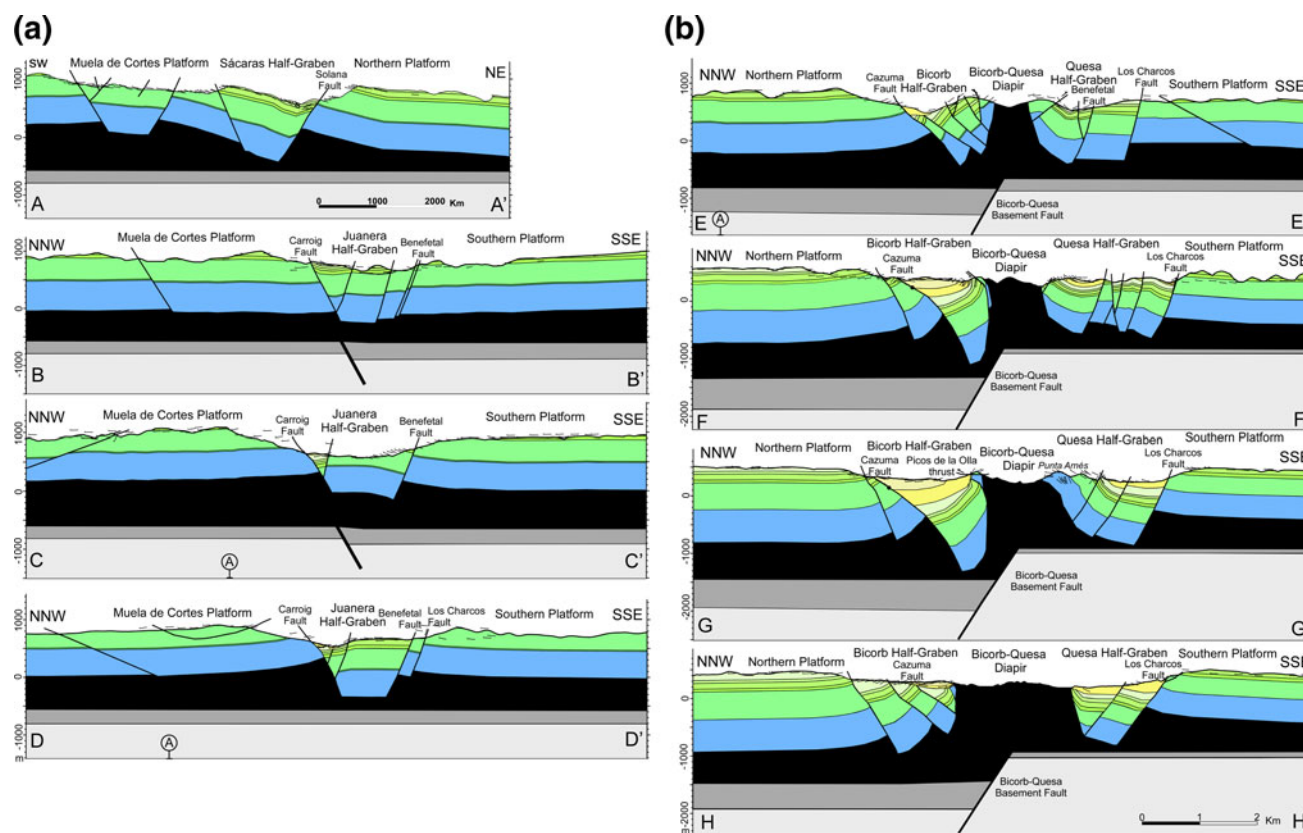


Fig. 7 West to East serial geological cross sections through the study area (see Fig. 5 for location) showing the decoupling of the deformation above and below the Middle-Upper Triassic evaporites.

faults bounding the Bicorb, Juanera and Sácaras Half-grabens (the Cazuma, Carroig and Solana Faults) where the Middle-Upper Triassic is up to 700 m thick (Fig. 7). In contrast, the thinning of the Middle-Upper Triassic beneath the half-grabens is especially conspicuous close to the Bicorb-Quesa diapir (the Bicorb, Quesa and western part of the Juanera Half-grabens) where this level seems to disappear completely. The origin of these changes in thickness should be attributed to the migration of the Keuper salt, which withdrew from under the thicker overburden areas to the areas where the overburden was thinner (in the Bicorb-Quesa Diapir and beneath the extensional faults creating reactive diapirs) (Vendeville and Jackson 1992; Nilsen et al. 1995). This fits in with the magnetotelluric data that show the presence of high resistive bodies (dry salt) in the Bicorb-Quesa Diapir and beneath the main half-graben bounding faults (Fig. 6).

Overburden structure

Northern segment (Sácaras Half-graben)

The Sácaras Half-graben system is located northwest of the western end of the Bicorb-Quesa Diapir (Fig. 4). It is a

Note the Bicorb-Quesa Diapir development on top of an N-dipping extensional basement fault and the overburden complex structure with both contractional and extensional faults on the diapir walls

half-graben that developed from the extensional motion of the SW-dipping Solana Fault and tilts 10–35° toward the NE of its hanging-wall overburden block (cross section AA' in Fig. 7). As in the other major extensional faults cutting the overburden (the Cazuma and Carroig Faults), this hanging-wall block is deformed close to the fault by a syncline whose geometry indicates that the overburden faulting was preceded by the growth of extensional fault-propagation folds. On the other side of the fault, which is the footwall block, the overburden is flexed up with a tilting that increases with the fault displacement (Fig. 7 cross section AA'). This flexure, which is also present in all major overburden-cutting faults, is ascribed to the inflation of Middle-Upper Triassic salt in the reactive diapirs that developed in the fault footwalls. The flexion also produces the bending of the overlying fault surface.

Western segment (Juanera Half-graben)

The Juanera Half-graben (Fig. 4) is bounded on the northwest by a SE-dipping extensional fault. This fault, the Carroig Fault, connects with the western end of the Bicorb-Quesa Diapir and depicts a dip slip which increases

eastwards up to 900–1,000 m close to this connection (cross sections CC' and DD' in Fig. 7). The horizontal arrangement of the Variscan basement top in the magnetotelluric I–I' profile (Fig. 6) shows that the Carroig fault is also rooted in the ductile Middle-Upper Triassic layer. However, the higher elevation of the subhorizontal overburden in the Muelas de Cortes platform with respect to the overburden located south of the Juanera Half-graben (cross sections CC' and DD' in Fig. 7) and the profile II–II' in Fig. 6 suggests that its location is controlled by the motion of an underlying buried basement fault.

The age of the Carroig Fault motion and of the Juanera Half-graben should be placed between the early-middle Miocene and the post-early-middle Miocene period. This is constrained by the presence of early to middle Miocene continental deposits in the hanging-wall fault block adjacent to the fault. These deposits are cut by the Carroig Fault and the related antithetic faults, whereas the underlying overburden is folded by the precursor extensional fault-propagation fold (syncline) (cross sections BB' to DD' in Fig. 7).

Earlier than this extensional deformation, no other Alpine deformations have been observed in the area, except close to the Bicornb-Quesa Diapir, where the unconformable arrangement of the lower-middle Miocene deposits over different Upper Cretaceous units (Fig. 4) points to the development of an ENE-trending Paleogene to earliest Miocene anticline. This anticline, which is located in the western prolongation of the Bicornb-Quesa Diapir, plunges westwards and disappears beneath the Juanera Half-graben infill (Fig. 5).

Eastern segment (Bicornb and Quesa Half-grabens)

The geological map (Fig. 4) and the cross sections EE' to HH' in Fig. 7 clearly show that the overburden structure in this rift segment is much more complex. In outline, it corresponds to two opposite-verging half-grabens (the Bicornb and Quesa Half-grabens) flanking a central anticline pierced by the Bicornb-Quesa Diapir.

The southeastern half-graben (*the Quesa Half-graben*) could be considered as the eastern extension of the Juanera Half-graben (Figs. 4, 5). The structural polarity of faulting and tilting is different in the two half-grabens. Unlike the Juanera Half-graben, the overburden here is mainly tilted to the southeast and the main bounding extensional fault is not located in the northwestern margin but in the southeastern one. This main extensional fault (Los Charcos Fault) dips northwestwards and connects westwards with the main antithetic fault of the Carroig Fault (the Benefetal Fault). The Los Charcos Fault increases its vertical throw to the east from 350 to 900 m (cross sections DD' to HH' in Fig. 7) while the footwall southeast tilting intensifies.

However, in the hanging-wall, the overburden is tilted to the southeast and compartmentalized by many NW-dipping extensional faults, among which is the eastern prolongation of the Benefetal Fault. This overburden, as in the Juanera Half-graben, is also unconformably overlain by Miocene successions. In the Quesa Half-graben, it is possible to distinguish two extensional events. The latter event involves all the Miocene materials, whereas the former involves the Lower-Middle Miocene (dated by Ruiz-Sánchez and Santisteban 2004) (Fig. 4 and cross section FF' in Fig. 7).

On the northern side of the Bicornb-Quesa Diapir, the *Bicornb Half-graben* consists of a NW-tilted block bounded northwards by SE-dipping extensional faults (cross sections DD' to HH' in Fig. 7). The main fault is the ENE-trending Cazuma Fault, which shows a dip slip of about 1000–1300 m, and is the highest of the half-graben main faults in the study area. Its large dip slip produces salt unloading below the fault and the rise of a reactive diapir, which folds the materials located above (Vendeville and Jackson 1992). In the footwall, north of the Cazuma Fault, there are minor faults parallel to the main one. These minor faults are less folded and present less displacement (Fig. 7 cross sections FF' and GG'). The Cazuma hanging-wall is NW-tilted and presents some minor extensional faults. On top of the Mesozoic materials, the Miocene sediments are disposed discordantly (Fig. 4 and 7 cross sections EE' to HH'). The lower-middle Miocene sediments are coeval with the extension of Cazuma Fault and with the hanging-wall faults, while the footwall faults are coeval with the upper Miocene sediments (Roca et al. 1996).

The serial cross sections in Fig. 7 clearly show that both the Mesozoic and the early-middle Miocene successions of the Bicornb and Quesa Half-grabens are bent up close to the Bicornb-Quesa Diapir. This bending-up is not symmetrical along the two diapir edges. It is much more pronounced along the northern diapir edge where the lower-middle Miocene appears vertical or even overturned. Along this edge, growth-strata geometries date the bending-up as middle Miocene, which is more or less coeval with the emplacement of the Picos de la Olla low-angle thrust (Roca et al. 1996). This NW-directed thrust, which is cut by the diapir, affects the lower-middle Miocene deposits but not the younger ones (Figs. 4, 7 cross section GG').

Before the development of these early-middle Miocene structures, the subcrop map in Fig. 8 clearly shows the presence of a pre-early-middle Miocene ENE-trending anticline in the present-day location of the Bicornb-Quesa Diapir that had been partially or totally eroded before the sedimentation of the Miocene deposits. This anticline, which is pierced by the Bicornb-Quesa Diapir, depicts a south-verging fold and has its hinge locally preserved on the southeastern flank of the diapir (Punta Arnés and

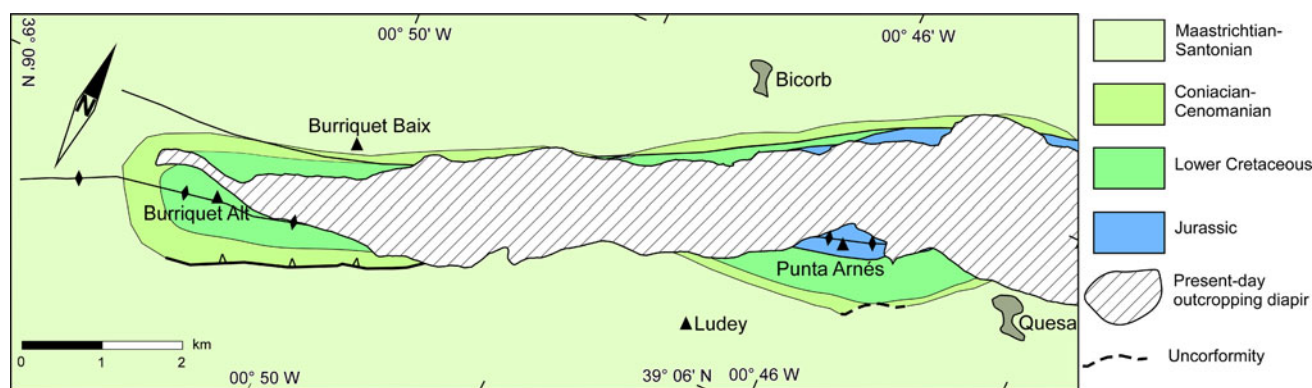


Fig. 8 Subcrop map of the Miocene showing the pre-diapiric structure of the study area

Burriquet Alt; Fig. 4). The Jurassic-Cretaceous successions folded by this anticline are thinner than in the rest of the study area and are cut by pre-Miocene faults (Fig. 7 cross sections EE' to HH'). These faults, in the forelimb (=northwestern part of the Quesa Half-graben), are high-angle SE-directed reverse faults formed during or after the anticline development. In contrast, in the backlimb (=southeastern part of the Bicorb Half-graben), they are, apparently, NW-directed reverse faults that are over-rotated faults and that, after unfolding the bent-up lower-middle Miocene deposits, became NW-dipping extensional faults. The age of the formation of these faults is probably assigned to the Mesozoic according to the models of Nalpas and Brun (1993), Vendeville et al. (1995), Withjack and Callaway (2000), Dooley et al. (2003). These models have the same configuration as our study area (basement, salt layer and overburden), and they show the formation of normal faults above the basement fault as well as the thinning of the overburden.

Bicorb-Quesa Diapir evolution

The comparative analysis of the overburden, Middle-Upper Triassic and Variscan basement structure shows that the Bicorb-Quesa Diapir developed above a NNW-dipping extensional basement fault with a complex deformational history that includes both contractional and extensional diapir reactivations. This story begins with the formation of a drape fold above the basement fault, which plays an essential role in the subsequent development of the area structure.

Specifically, our structural observations, combined with the tectono-sedimentary information provided by the Miocene deposits (Roca et al. 1996; Anadón et al. 1998), allow us to establish that the present-day structure of the Bicorb-Quesa Diapir is the result of a complex Alpine evolution with six major deformational stages. The first three stages are linked to the Mesozoic extensional opening

of the Tethys Sea and the other three to the development of the Iberian and Betic thrust-and-fold belts (Fig. 9).

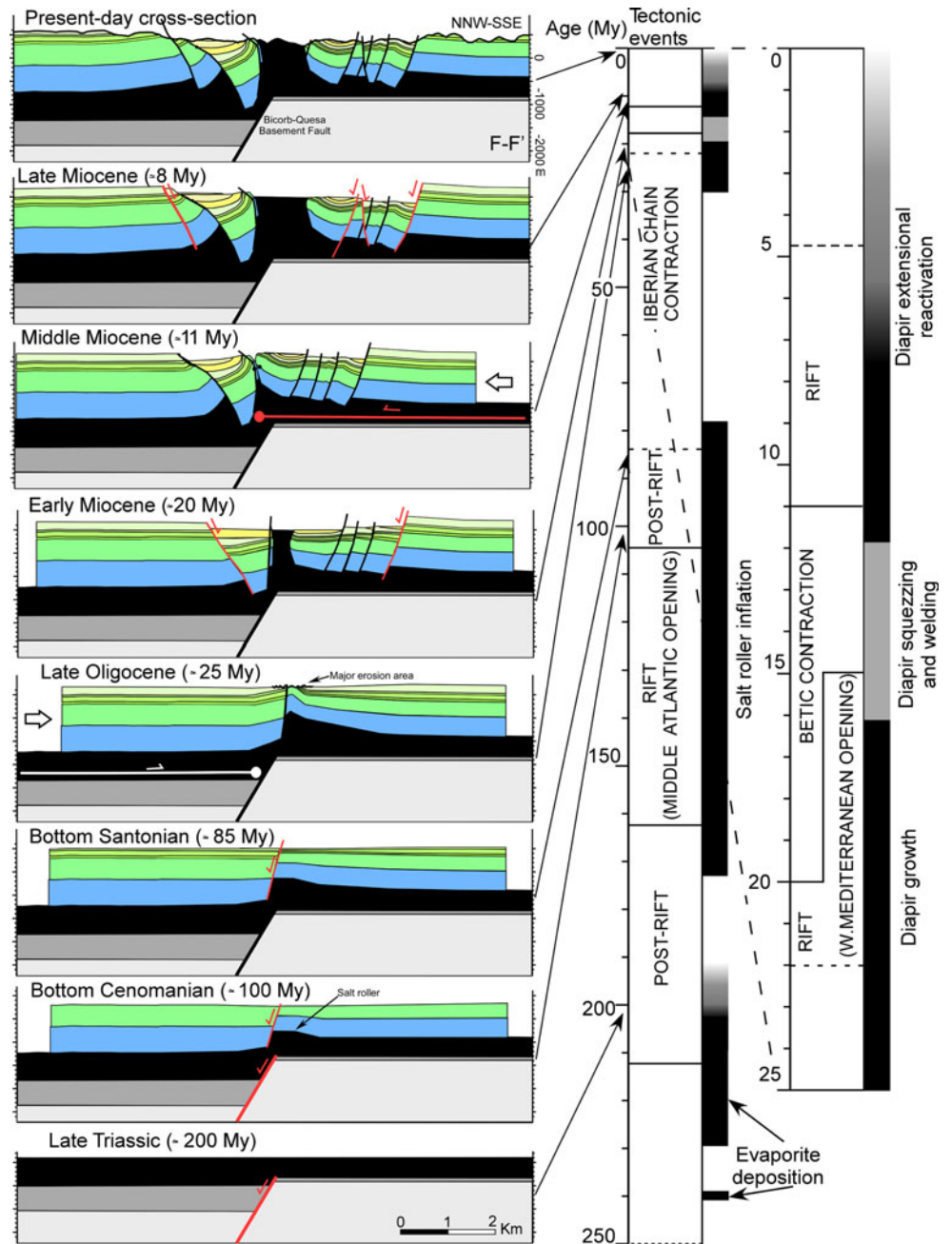
Permian-Early Triassic rift stage

This is the first Alpine deformational stage observed in the study area, and it corresponds to the extensional stage in which the NNW-dipping Bicorb-Quesa basement fault was formed. The extensional motion of this fault during the Permian-Early Triassic period is evidenced by the variations in thickness of the pre-Jurassic successions which, according to the magnetotelluric data, are much thicker in its hanging-wall (1100 m) than in its footwall (600 m). The parallel extensional basement fault depicted in Fig. 2 beneath the Xúquer Diapir probably also formed during this rifting stage.

Late Jurassic-early Cretaceous synrift stage

Although most of the extensional motion of the Bicorb-Quesa Fault occurred during the Permian-Early Triassic period, variations in thickness of the Mesozoic overburden indicate that this fault also moved extensionally during the sedimentation of the Upper Jurassic-Lower Cretaceous successions. However, this motion, which was much smaller, produced the monoclinical drape folding of the overburden over the basement extensional fault, with salt accommodating the difference in geometry (Fig. 9). The extension of this folded overburden probably led to the formation of the extensional fault recognized on the northern flank of the present-day Bicorb-Quesa Diapir. This motion could have generated other extensional faults on the northern flank, but they cannot be identified given that they were rejuvenated in later events. These extensional faults, which developed at the upper hinge of the monoclinical drape fold, would contribute to the formation of an incipient reactive diapir (a salt roller) with salt provided by both the hanging-wall and the footwall (Burliga et al. 2012).

Fig. 9 Partial restorations of the F–F' transverse cross section showing the main structural features of the Biorb-Quesa rift system at the main Alpine deformational stages affecting the eastern Iberian plate (see Fig. 5 for location and Fig. 3 for legend)



Upper Cretaceous postrift stage

The extensional motion of the Biorb-Quesa Fault and the related overburden deformation ended before the start of the Upper Cretaceous. The Cenomanian and Turonian successions are affected only by a slight thinning in the footwall of the active extensional fault that developed at the upper hinge of the previously formed monoclinical drape fold. The Cenomanian-Turonian materials go from the regular thickness of 200–80 m in this area (Fig. 7 cross section EE' to HH'). Formed in an extensional regional postrift setting (Salas and Casas 1993; Salas et al. 2001),

this thinning is interpreted as being driven by a still-working migration of the Middle-Upper Triassic salt because of the overburden load differences (Ge et al. 1997).

Paleogene contractional stage

Between the Senonian (Upper Cretaceous) and the early Miocene, the previous thinning area (the reactive diapir) becomes an S-verging anticline with fairly vertical limbs and a positive relief of between 200 and 400 m over the region (Fig. 9 and cross section EE' to FF' in Fig. 7). This

anticline is well recorded in the lower-middle Miocene subcrop map (Fig. 8). It is detached on the Middle-Upper Triassic evaporite layers and had its southern limb cut by S-directed reverse faults. The fold shape, the relief and the presence of the reverse fault rule out the possibility that it was formed by extension, while the lack of active diapirism enables us to conclude that the fold is formed by rejuvenation. These rejuvenation folds are well known in thick-skinned deformations in a contractive event (Letouzey et al. 1995; Krzywiec 2004; Ferrer et al. 2012). Moreover, not far from the study area stands the Iberian Chain (Paleogene and earliest Miocene) (Fig. 1). In these nearby areas, the Iberian Chain is formed by a thrust-and-fold system detached above Middle-Upper Triassic salts that propagated southeastwards through time. As shown in the cross section in Fig. 2, the location of the deformational front of this part of the Iberian Chain is controlled by the presence of pre-existing basement faults (in this case, the Xúquer basement fault), which cut and displaced the Middle-Upper Triassic detachment level. In this regional scenario, the Paleogene anticline that developed in the Bicornb-Quesa area can be attributed to a further propagation of the Iberian Chain deformation above the Middle-Upper Triassic level of the footwall block of Xúquer basement fault. Further propagation was hampered by the Bicornb-Quesa Fault, which displaced the detachment level, resulting in the formation of a new frontal fold above this sticking point.

Early-middle Miocene diapiric stage

The Bicornb-Quesa Diapir became active and rose to the crest of this anticline just before or at the start of the sedimentation of the lower-middle Miocene detrital deposits. This is evidenced by the petrological composition of the deposits (Roca et al. 1996). The origin of this precursor Bicornb-Quesa Diapir has been explained by the denudation of extensional faulting caused by the opening of the Valencia Trough (Roca et al. 1996, 2006). However, the diapir rise also seems related to the erosion of the anticline rejuvenated during the Paleogene contractional stage, which was significantly eroded before the deposition of the lower-middle Miocene sequences (Fig. 9). The growth of the Bicornb-Quesa Diapir during the early-middle Miocene entailed salt evacuation on the hanging-wall block of the Bicornb-Quesa Fault and, to a lesser extent, in the other diapir areas. This resulted in the sinking of the overlying overburden, which was extensionally faulted and unconformably overlain by relatively thick lower-middle Miocene detrital successions. Coeval with this process, the Bicornb and the incipient Quesa and Juanera Half-grabens were formed as salt evacuation basins.

Middle Miocene contractional stage

During the Middle Miocene development of the Prebetic folds and thrusts, the pre-existing Bicornb-Quesa Diapir was shortened producing, first, the squeezing of the diapir as indicated in the sedimentary record by a significant rise of evaporitic material (Roca et al. 1996). Then, once the diapir was welded, a contractional deformation occurred in the surrounding overburden and lower-middle Miocene syndiapir rocks (Roca et al. 1996, 2006; Fig. 9). This contractional deformation was focused on the pre-existing diapir because of its weakness, and it consisted of a major NNW-verging anticline cut on its forelimb by the NNW-directed Picos de la Olla low-angle thrust. This contractive event could be responsible for the thrust observed inside the present-day diapir. As in the Paleogene contractional stage, the Middle Miocene contractional deformation did not affect the basement since it was detached from the Middle-Upper Triassic evaporites. However, the deformation during this shortening phase propagated northwards in the footwall of the Bicornb-Quesa basement fault (Fig. 9). This different configuration hampers the propagation of Prebetic thin-skinned contractional deformation north of the Bicornb-Quesa basement fault because the detachment level was down-dropped to the north of the fault.

Late Miocene extensional diapir reactivation stage

This is the last Alpine deformational stage distinguished in the study area. It corresponds to a regional extensional stage in which the Jurassic-Cretaceous subhorizontal platform of the Valencian Domain was extended by means of the formation of several sets of extensional faults detached in the Middle-Upper Triassic evaporites (De Ruig 1992, Roca et al. 1996; Fig. 9). In the study area, this extensional overburden deformation produced the extensional reactivation of the squeezed Bicornb-Quesa Diapir and the development, at its western prolongation, of a major SE-dipping extensional fault (the Carroig Fault) (Roca et al. 1996, 2006).

The role of pre-existing basement faults in the initiation and reactivation of salt diapirs

The reconstruction of the evolution of the Bicornb-Quesa Diapir indicates a complex salt diapir that evolved from a contractional and extensional thin-skinned deformation of an overburden located on top of a pre-existing extensional basement fault. A thin-skinned deformation produced the rejuvenation of a previous reactive diapir, the growth of the Bicornb-Quesa Diapir, the squeezing of the diapir and the reactivation of the diapir.

In each of these stages, cover deformation and diapirism appear strongly influenced by the propagation direction of the deformation above the detachment level, which was previously flexed or truncated on top of the pre-existing basement fault. This propagation, in the compressive stages, was directed toward the basement fault. In the Paleogene contractional stage, it occurred in the hanging-wall, whereas in the middle Miocene, it occurred in the footwall. Below we discuss the role played by the pre-existing basement faults in the thin-skinned contractional initiation and reactivation of salt diapirs, focusing on the influence of the propagation direction of the cover deformation.

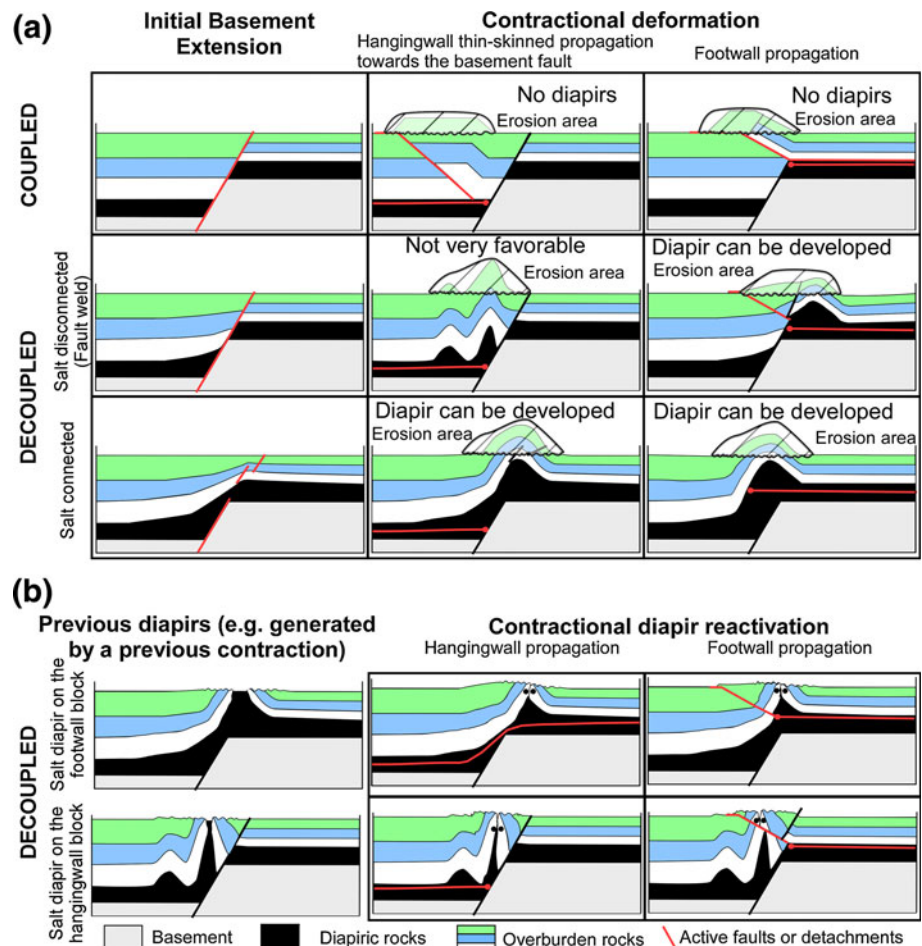
Contractional diapir initiation

Before addressing contractional deformation, it should be noted that the structural style of overburden and salt-layer deformation above a growing extensional basement fault is strongly dependent on the degree of decoupling between supra- and subsalt deformation (Withjack and Callaway 2000). Thus, if the deformation is coupled, then the deformation style is transferred through the detachment level

(Fig. 10). By contrast, if the deformation is decoupled, structural styles above and below the salt can be quite different and may result in an overburden drape folding above a basement extensional fault (Jackson and Vendeville 1994). Since the overburden section must extend as much as the basement, this drape folding is accompanied by extensional faulting on the upper hinge of the monoclinial drape fold. This is the area where reactive diapirs can initiate (Fig. 10). Also in this decoupled scenario, salt-layer thickness is not constant but changes laterally, accommodating the difference between the supra- and subsalt geometries. As regards this major salt mobility, the salt layer (potential future detachment level of later thin-skinned deformations) usually has lateral continuity above the basement fault, which does not occur in the coupled scenario, where it is simply cut and displaced by the fault (Fig. 10).

Shortening of these different thick-skinned salt tectonic structures would promote the growth of different contractional structures (mainly folds) which, in some cases, can enhance diapirism as a result of their erosion and/or fracture weakening (Fig. 10). The diapir initiation in these structures would not only depend on the amount of overburden denudation but also on the fold shape and

Fig. 10 Summary diagram of the role of pre-existing extensional basement faults in the cover thin-skinned contractional initiation (a) and reactivation (b) of salt diapirs. The analysed factors are the propagation sense and the degree of coupling or decoupling of the thin-skinned deformation



kinematics. This initiation also depends of the following factors: thickness and mechanical behaviour of the overburden, deformation rates, amount of deformation, thickness of the salt, the pre-existing overburden, salt configuration, etc. Consequently, the possibility of developing contractional-driven diapirism over a pre-existing basement fault will be different if the contractional deformation is developed over a previously coupled or decoupled overburden. The resulting structure will also depend on whether the overburden thin-skinned contractional deformation propagates on top of the hanging-wall or on top of the footwall of the basement fault.

We focus on three possible scenarios: (1) a coupled salt layer, (2) a decoupled salt layer with the footwall and hanging-wall salt layer that is disconnected and (3) a decoupled salt layer that is connected (Fig. 10a). Thus, if we consider that the salt layer acts as a detachment level, the contractional deformation can be propagated toward the pre-existing extensional basement fault over its hanging-wall or over its footwall (Fig. 10a).

In the case of a salt-disconnected/hanging-wall propagation, the basement fault acts as a barrier for the propagation of the contractional overburden deformation, leading to the development of buttressing structures (mainly detachment folds and backthrusts) or basement short cuts. In this setting, the salt-cored structures that developed from contractional structures have a thick overburden and, therefore, are not very suitable for being pierced by salt. The only exception might be the tight buttress anticlines that can be formed against the fault plane (Fig. 10a). These anticlines present better conditions for developing a salt diapir since they tend to be taller and have an initial small overburden/salt thickness ratio (see above for more information on a decoupled extensional deformation over a basement extensional fault). Furthermore, if a basement short cut develops, these anticlines could also be significantly uplifted above the regional level, favouring a deep erosion to an even greater extent.

In the case of a salt-connected/hanging-wall propagation, the overburden contractional deformation can propagate toward the basement fault footwall above the inherited flat-ramp-flat geometry of the upper part of the salt layer. This detachment geometry leads to the development of a detachment fold on the concave-downward detachment bend, and also to the squeezing of the salt located on the basement fault surface. The salt is expelled upwards toward the generated detachment fold. Note that all these contractional structures develop at or very close to the location of the hinge of the overburden monoclinical drape fold that formed during the older extensional motion of the underlying basement fault. Therefore, contractional anticlines develop at the place where the overburden is thinner and

where the salt layer is thicker (Fig. 10a). As a result, the formation of diapirs by erosion and salt breakthrough is relatively easy here. An example of this kind of contractional-driven diapir would be the one that developed during the Paleogene-Lower Miocene over the Bicorb-Quesa basement fault.

In the case of a footwall propagation, the contractional deformation would be blocked at the top of the basement fault. The detachment fault would be interrupted by the fault in a salt-disconnected scenario or by the monocline limb of the drag fold in a salt-connected scenario. This would give rise to the formation of a thrust front or detachment anticline at the top of the basement footwall cut-off of the pre-existing extensional fault (Fig. 10a). As in the previous case, these contractional structures would be developed at or very close to the hinge of the overburden monoclinical drape fold that formed during the older extensional motion of the underlying basement fault. Consequently, they would also constitute a suitable location for the generation of salt diapirs by overburden denudation. The Betic Front at the Xúquer River (Fig. 2) provides an example of this kind of situation.

Contractional diapir reactivation and/or squeezing

The propagation direction of an overburden contractional deformation also plays a major role in the contractional reactivation and/or squeezing of a salt diapir developed over an extensional basement fault. Both the geometrical features and the evolutionary trends of shortened diapirs will be rather different depending on whether the contractional deformation propagates toward the diapir over the hanging-wall or over the footwall of the basement fault (Fig. 10b).

Indeed, if contractional deformation propagates above the salt layer lying over the hanging-wall block, the entire pre-existing diapir narrows, forcing a large volume of salt to flow upwards. This results in an acceleration of the extrusion of diapiric materials or, in the case of a buried diapir, in its rejuvenation. With increased shortening, the diapirs close along secondary welds or generated “Q-tip” structures (Rowan and Vendeville 2006; Dooley et al. 2009). Folds and thrusts form at the squeezed diapir limb with a predominant vergence that will depend on the basement fault dip. Note that this evolution is only valid if the overburden contractional deformation can propagate up to the salt diapir location above a continuous detachment salt layer (see discussion on the propagation of overburden deformation above a basement fault in the previous section). In the other cases, diapir reactivation will be more difficult and complex (e.g. diapirs developed over the basement fault but disconnected from the source layer by a primary weld), or it may never occur (diapirs developed

over the basement footwall block in a pre-contractonal configuration in which the detachment salt layer has a high-angle dip above the basement fault).

In the case where contractional overburden deformation has propagated on the basement footwall block, all pre-existing salt diapirs can be easily reactivated, provided that primary welds were formed on their flanks (Fig. 10b). The pattern of the contractional reactivation in pre-existing diapirs is similar to the pattern described in the previous scenario with the exception of diapirs that developed over the basement fault surface. In these scenarios, not all the diapir is shortened but only part of the feeding stem located above the detachment level of the regional footwall of the basement fault. Moreover, the postdiapir welding thrusts and folds in these diapirs show a preference for vergence toward the foreland, with the development of forethrusts in the diapir forelimb (Fig. 10). It is interesting to note that the preservation of the lower part of the feeding stems in these diapirs can favour later diapir reactivation, even where the upper part of the diapir was completely welded. An example of this kind of later reactivation is the Bicornb-Quesa Diapir, which was contractionally welded during the middle Miocene and reactivated during the late Miocene by extensional thinning of the overburden above the welded stem or feeder.

Conclusions

Detailed analysis of structural surface data in addition to available and new magnetotelluric data enabled us not only to recognize the structure and Alpine evolution of the Bicornb-Quesa Diapir but also to propose a new model for contractional diapir initiation and reactivation over a pre-existing extensional basement fault.

In the study area, the geometric analysis of the available data indicates that the Alpine structure of the Bicornb-Quesa area is strongly conditioned by the presence of a ductile and diapiric Middle-Upper Triassic level. The evaporite-detrital level decouples the deformation of the Iberian basement from the one affecting the Jurassic to Miocene overburden. This leads to a structural style of deformation of the basement (thick-skinned) and overburden (thin-skinned) that is completely different from the structural style especially during Cenozoic times, when contractional and extensional deformations only affected the overburden.

The Bicornb-Quesa Diapir is a salt wall formed above an NNW-dipping extensional basement fault with a complex deformational history that includes both contractional and extensional diapir reactivations. The extensional basement fault formed during Permian-Early Triassic times and still slightly active up to the beginning of the Late Cretaceous produced the development of a monoclinical drape fold in

the Jurassic-Cretaceous overburden as well as the formation of a reactive diapir on the hinge of the drape fold. After the Late Cretaceous, the Jurassic-Cretaceous overburden was affected by thin-skinned contraction related to the formation of the Iberian Chain and Betics. These deformations led to the polyphase development of the Bicornb-Quesa Diapir because of the erosion of a Paleogene rejuvenated reactive diapir on top of the basement fault, and because of the early Miocene extension. This diapir was contractionally deformed during the middle Miocene and extensionally reactivated during the late Miocene.

The role played by pre-existing basement faults in thin-skinned contractional initiation and reactivation of salt diapirs was analysed using the information provided from this reconstruction. This analysis highlights the role played by the geometric relationship between the propagation direction of the cover deformation and the dip direction of the basement fault. In this regard, it shows that (1) the propagation of an overburden contractional deformation over a basement footwall block results in the development of detachment folds on top of the basement fault which, with a thin cover, are propitious for the formation of a salt diapir by erosion, and (2) the propagation of an overburden contractional deformation over the basement hanging-wall block is not very favourable to the formation of salt diapirs since it generally induces the generation of buttressing structures that involve a thicker hanging-wall sequence that resists piercement. This general working model, however, is not without its exceptions. The main exception is attributed to the presence of a thick salt layer beneath the monocline drape fold. A thick salt layer, when squeezed by a hanging-wall compressive deformation, can displace salt to the footwall block and pump up the reactive diapir, allowing the diapir to grow.

As for diapir reactivation, when a contractional deformation propagates toward a pre-existing diapir over the hanging-wall, it will result in the entire narrowing of pre-existing diapirs over the basement fault but not in the entire narrowing of the ones located over the basement footwall block. By contrast, a footwall propagation of the contractional deformation will generate the entire narrowing of all pre-existing diapirs over the footwall block, but only a portion of the diapirs formed over the basement fault. Specifically, in these diapirs, the lower part of the stems remains almost undeformed, creating a situation very propitious for a subsequent diapir reactivation even if the upper part of the diapir is completely welded.

Acknowledgments This work was funded by the project INTEC-TOSAL (CGL2010-21968-C02-01) of the Ministerio de Educación y Ciencia, the “Grup de Recerca de Geodinàmica i Anàlisi de Conques” (2005SGR-000397) and (PIER-CO2 CGL2009-07604). Midland Valley is gratefully acknowledged for providing software. We are very indebted to reviewers Tim Dooley, Menno de Ruig and Reinhard Greiling for improving an early version of the manuscript.

References

- Álvarez M, Capote R, Vegas R (1979) Un modelo de evolución geotectónica para la Cadena Celtibérica. *Acta Geol Hisp* 14:172–177
- Anadón P, Robles F, Roca E, Utrilla R, Vázquez A (1998) Lacustrine sedimentation in the diapir-controlled Miocene Bicorn basin, eastern Spain. *Palaeogeogr Palaeoclimatol Palaeoecol* 140:217–243
- Anadón P, Utrilla R, Vázquez A (2000) Use of charophyte carbonates as proxy indicators of subtle hydrological and chemical changes in marl lakes: example from the Miocene Bicorn Basin, eastern Spain. *Sediment Geol* 133:325–347
- Arche A, Lopez-Gomez J (1996) Origin of the Permian-Triassic Iberian Basin, central-eastern Spain. *Tectonophysics* 266:443–464
- Arche A, Diez JB, López-Gómez J (2007) Identification of the Early Permian (Autunian) in the subsurface of the Ebro Basin, NE Spain, and its paleogeographic consequences. *J Iber Geol* 33(1):125–133
- Azéma J, Foucault A, Chauve P, Fourcade E, García-Hernández M, González-Donoso JM, Linares A, Linares D, López-Garrido AC, Rivas P, Vera JA (1979) Las microfácies del Jurásico y Cretácico de las Zonas Externas de las cordilleras Béticas. *Publ Univ Granada*
- Bartrina T, Hernández E, Serrano A (1990) Estudio de subsuelo del Trias salino en la Depresión Intermedia. In: Ortí F, Salvany JM (eds) Formaciones evaporíticas de la Cuenca del Ebro y cadenas periféricas y de la zona de Levante. ENRESA—Univ de Barc, pp 232–238
- Blumenthal M (1927) Versuch einer tektonischen gliederung der betischen cordilleren von Central, und Sud-West Andalusien. *Eclogae Geol Helv* 20:487–592
- Burliga S, Koyi H, Chemia Z (2012) Analogue and numerical modelling of salt supply to a diapiric structure rising above an active basement fault In: Alsop GI, Archer SG, Hartley AJ, Grant NT, Hodgkinson R (eds) Salt Tectonics, Sediments and Prospectivity, vol 363. Geological Society, London (special publications), pp 395–408
- Callot JP, Jahani S, Letouzey J (2007) The role of pre-existing diapirs in fold and thrust belt development. In: Lacombe O, Lavé J, Roure F, Verges J (eds) Thrust belts and foreland basins: from fold kinematics to hydrocarbon systems. Springer, Berlin, pp 309–325
- Carbó A (1980) Investigación geotectónica en el borde suroriental de la Cordillera Ibérica (prov. de Valencia y Albacete), basada en determinaciones gravimétricas. Tesis Doctoral, Univ. Complutense Madrid
- Carbó A (1982) Estructura cortical del Levante Español en base a datos gravimétricos. *Real Acad Cien Exac Fis Nat* 76(2):365–378
- Castaño S, Carbó A (1995) Los afloramientos triásicos de la zona de confluencia de las Cordilleras Ibérica y Bética. Aportes de la gravimetría a su interpretación. *Cuad de Geol Ibér* 19:235–248
- Coward M, Stewart S (1995) Salt-influenced structures in the Mesozoic–Tertiary cover of the southern North Sea, UK. In: Jackson MPA, Roberts DG, Snelson S (eds) Salt tectonics: a global perspective, vol 65. American Association of Petroleum Geologists, Memoirs, pp 229–250
- De Ruijg MJ (1992) Tectono-sedimentary evolution of the prebetic fold belt of Alicante (SE Spain) a study of stress fluctuations and foreland basin deformation. PhD thesis, Structural geology and tectonics group. Vrije Universiteit, Amsterdam
- De Ruijg MJ (1995) Extensional diapirism in the eastern Prebetic foldbelt, southeastern Spain. In: Jackson MPA, Roberts DG, Snelson S (eds) Salt tectonics: a global perspective, vol 65. American Association of Petroleum Geologists, Memoirs, pp 353–367
- De Torres T, Sánchez A (1990) Espesores de las facies Keuper en la Rama Castellana del la Cordillera Ibérica y en el Dominio Prebético. In: Ortí F, Salvany JM (eds) Formaciones evaporíticas de la Cuenca del Ebro y cadenas periféricas y de la zona de Levante. ENRESA, Univ de Barc, pp 212–218
- Dooley T, McClay KR, Pascoe R (2003) 3D analogue models of variable displacement extensional faults: applications to the Revfallet fault system, offshore mid-Norway. In: Nieuwkand DA (ed), New insights into structural interpretation and modelling, vol 212. Geological Society, London (special publications), pp 151–167
- Dooley T, McClay KR, Hempton M, Smit D (2005) Salt tectonics above complex basement extensional fault systems: results from analogue modeling. In: Doré AG, Vining BA (eds) Petroleum geology: north-west Europe and global perspectives-proceedings of the 6th petroleum geology conference. Geological Society of London, pp 1631–1648
- Dooley TP, Jackson MPA, Hudec MR (2009) Inflation and deflation of deeply buried salt stocks during lateral shortening. *J Struct Geol* 31:582–600
- Ferrer O, Jackson MPA, Roca E, Rubinat M (2012) Evolution of salt structures during extension and inversion of the offshore Parentis Basin (Eastern Bay of Biscay) In: Alsop GI, Archer SG, Hartley AJ, Grant NT, Hodgkinson R (eds) Salt tectonics, sediments and prospectivity, vol 363. Geological Society, London, (special publications), pp 361–380
- García A, García L, Muelas A et al (1981) Mapa geológico de España 1:50.000, Llobat. IGME, Madrid
- García-Hernández M, López-Garrido AC, Rivas P, Sanz de Galdeano C, Vera JA (1980) Mesozoic palaeogeographic evolution of the external zones of the Betic Cordillera. *Geol Mijnbouw* 59:155–168
- García-Rodrigo B (1960) Sur la structure du Nord de la province d'Alicante (Espagne). *Bull Soc Géol Fr* 7:273–277
- Ge H, Jackson MPA, Vendeville BC, Maler MO, Handschy JW (1997) Deformation of prograding wedges over a ductile layer—applications of physical models to geologic examples. *Gulf Coast Assoc Geol Soc Trans* 47:177–184
- Groom RW, Bailey RC (1989) Decomposition of the magnetotelluric impedance tensor in the presence of local three-dimensional galvanic distortion. *J Geophys Res* 94:1913–1925
- Guimerà J, Álvaro M (1990) Structure et evolution de la compression alpine dans le Chaîne Iberique et la Chain Cotiere Catalan (Espagne). *Bull Soc géol Fr* 8:339–340
- Guimera J, De Vicente G, Rodriguez Pascua MA (2004) La Rama Castellano-Valenciana. In: Vera JA (ed) Geología de España. SGE-IGME, Madrid, pp 610–612
- Jackson MP, Vendeville B (1994) Regional extension as a geologic trigger for diapirism. *Geol Soc Am Bull* 106:57–73
- Krzywiec P (2004) Triassic evolution of the Klodawa salt structure: basement-controlled salt tectonics within the Mid-Polish trough (Central Poland). *Geol Q* 48:123–134
- Lanaja JM (1987) Contribución de la exploración petrolífera al conocimiento de la Geología de España. IGME, Madrid
- Letouzey J, Colletta B, Vially R, Chermette JC (1995) Evolution of salt related structures in compressional setting. In: Jackson MPA, Roberts DG, Snelson S (eds) Salt tectonics: a global perspective, vol 65. American Association of Petroleum Geologists, Memoirs, pp 41–60
- Martínez del Olmo W (1999) Diapirismo de sales triásicas: consecuencias estructurales y sedimentarias en el Prebético Oriental, (Cordillera Bética, SE de España). In: Buergo EA, Merten R, Villalobos L, Varela J (eds) Libro Homenaje a José Ramírez del Pozo. AGGP, Madrid, pp 175–187

- Martínez-Poyatos D, Gutiérrez Marco JC, Pardo Alonso MV, Rábano I, Sarmiento GN (2004) La secuencia paleozoica postcámbrica. In: Vera JA (ed) *Geología de España*. SGE-IGME, Madrid, pp 81–83
- McNeice GW, Jones AG (2001) Multisite, multifrequency tensor decomposition of magnetotelluric data. *Geophysics* 66:158–173
- Meléndez A (1979) El Cretácico del Macizo de Caroch (provincias de Valencia y Albacete). *Cuad Geol Ibér* 5:435–452
- Moissenet E (1985) Les dépressions tarditectoniques des Chaînes Ibériques méridionales: distension, diapirisme et dépôts neogènes associés. *C R Ades Sci Paris* 300:523–528
- Nalpas T, Brun JP (1993) Salt flow and diapirism related to extension at crustal scale. *Tectonophysics* 228:349–362
- Nilsen KT, Vendeville BC, Johansen JT (1995) Influence of regional tectonics on halokinesis in the Nordkapp Basin, Barents Sea. In: Jackson MPA, Roberts DG, Snelson S (eds) *Salt tectonics: a global perspective*, vol 65. American Association of Petroleum Geologists, Memoirs, pp 413–436
- Ortí F (1974) El Keuper del Levante español. *Estud Geol* 30:7–46
- Ortí and Salvany (1990) Formaciones evaporíticas de la Cuenca del Ebro y Cadenas periféricas y de la zona de Levante. ENRESA, Barcelona
- Ott d'Estevou P, Montenat Ch, Ladure F, Pierson d'Autrey L (1988) Évolution tectono-sédimentaire du domaine prébéétique oriental (Espagne) au Miocène. *C R Acad Sci Paris* 307:789–796
- Ríos JM, Beltrán FJ, Zapatero MA, Goy JL, Zazo C, Martínez C (1980) Mapa Geológico de España 1:50.000, Navarrés. IGME, Madrid
- Roca E, Anadón P, Utrilla R, Vázquez A (1996) Rise, closure and reactivation of the Biorb-Quesa diapir, eastern Prebetics, Spain. *J Geol Soc Lond* 153:311–321
- Roca E, Sans M, Koyi H (2006) Polyphase deformation of diapiric areas in models and in the eastern Prebetics (Spain). *Am Assoc Pet Geol Bull* 90:115–136
- Rowan MG, Vendeville BC (2006) Foldbelts with early salt withdrawal and diapirism: physical model and examples from northern Gulf of Mexico and the Flinders ranges, Australia. *Mar Pet Geol* 23(9–10):871–891
- Rubinat M, Ledo J, Roca E, Rosell O, Queralt P (2010) Magnetotelluric characterization of a salt diapir: a case study on Biorb-Quesa Diapir (Prebetic Zone, SE Spain). *J Geol Soc Lond* 167:145–153
- Ruiz-Sánchez FJ, Santisteban C (2004) Tres nuevas localidades con fauna de micromamíferos fósiles de edad Aragoniense inferior-medio en el sector sureste de la cuenca de Quesa-Biorb (prov. de Valencia, España). *Geogaceta* 35:123–125
- Salas R, Casas A (1993) Mesozoic extensional tectonics, stratigraphy and Alpine cycle of the Eastern Iberian basin. *Tectonophysics* 228(1–2):33–55
- Salas R, Guimerà J, Mas R, Martín-Closas C, Meléndez A, Alonso A (2001) Evolution of the Mesozoic Central Iberian Rift system and its Cainozoic inversion (Iberian Chain). In: Ziegler PA, Cavazza W, Robertson AFH, Crasquin-Soleau S (eds) *Peri Tethyan rift/wrench basins and passive margins*, vol 186. Muséum National d'Histoire Naturelle, pp 145–185
- Sans M, Koyi HA (2001) Modeling the role of erosion in diapir development in contractional settings. In: Koyi HA, Mancktelow NS (eds) *Tectonic modeling: a volume in honor of Hans Ramberg*, vol 193. Geological Society of America Memoir, pp 111–122
- Santisteban C, Ruiz-Sánchez FJ, Bello D (1989) Los depósitos lacustres del Terciario de Biorb (Valencia). *Acta Geol Hisp* 24:299–307
- Santisteban C, Ruiz-Sánchez FJ, Lacombra JI (1994) Estratigrafía, edad y evolución de los depósitos terciarios de la cuenca de antepaís de Quesa-Biorb (Valencia). *Comunicaciones al II Congreso del Grupo Español del Terciario*, Jaca, pp 209–212
- Simpson F, Bahr K (2005) *Practical Magnetotellurics*. Cambridge University Press, Cambridge
- Sopeña A, Sánchez-Moya Y (2004) Las cuencas continentales del fin de la Orogenia Varisca. In: Vera JA (ed) *Geología de España*. SGE-IGME, Madrid, pp 479–481
- Suarez Alba J (2007) La Mancha Triassic and lower Lias stratigraphy, a well log interpretation. *J Iber Geol* 33(1):55–78
- ter Borgh MM, Oldenhuis R, Biermann C, Smit JHW, Sokoutis D (2011) The effects of basement ramps on deformation of the (Spain): a combined field and analogue modeling study. *Tectonophysics* 502:62–74
- Vendeville BC, Jackson MPA (1992) The rise of diapirs during thin-skinned extension. *Mar Pet Geol* 9(4):331–353
- Vendeville BC, Nilsen KT (1995) Episodic growth of salt diapirs driven by horizontal shortening. In: Travis CJ, Vendeville BC, Harrison H, Peel FJ, Hudec MR, Perkins BJ (eds) *Salt, sediment and hydrocarbons: Gulf Coast Section SEPM Foundation 16th annual research conference*, pp 285–295
- Vendeville BC, Hongxing G, Jackson MPA (1995) Scale models of salt tectonics during basement-involved extension. *Pet Geosci* 1:179–183
- Vera JA (1983) Las Zonas Externas de la Cordillera Bética. In: Comba JA (ed) *Geología de España, Libro Jubilar JM Ríos*, vol 1. IGME, Madrid, pp 218–251
- Vozoff K (1991) The magnetotelluric method. In: Nabighian MN (ed) *Electromagnetic methods in applied geophysics*, vol 2B. Society of Exploration Geophysicists, Tulsa, OK, pp 641–711
- Withjack M, Callaway S (2000) Active normal faulting beneath a salt layer: an experimental study of deformation patterns in the cover sequence. *Am Assoc Pet Geol Bull* 85:627–651